

# The influence of hydrostatic pressure on tissue engineered bone development

K.H.L. Neßler<sup>a,b</sup>, J.R. Henstock<sup>c,d</sup>, A.J. El Haj<sup>d</sup>, S.L. Waters<sup>e</sup>, J.P. Whiteley<sup>b</sup>, J.M. Osborne<sup>b,f,\*</sup>

<sup>a</sup>Department of Mathematics, University of Kaiserslautern, Postfach 3049, 67653 Kaiserslautern, Germany

<sup>b</sup>Department of Computer Science, University of Oxford, Wolfson Building, Parks Road, Oxford OX1 3QD, UK

<sup>c</sup>Institute of Ageing and Chronic Disease, University of Liverpool, Apex Building, West Derby Street, Liverpool L7 8TX, UK

<sup>d</sup>Institute for Science & Technology in Medicine, Keele University, Guy Hilton Research Centre, Thornburrow Drive, Hartshill, Stoke-on-Trent ST4 7QB, UK

<sup>e</sup>Mathematical Institute, University of Oxford, Andrew Wiles Building, Radcliffe Observatory Quarter, Woodstock Road, Oxford OX2 6GG, UK

<sup>f</sup>School of Mathematics and Statistics, University of Melbourne, Parkville, Victoria 3010, Australia

---

## Abstract

The hydrostatic pressure stimulation of an appropriately cell-seeded porous scaffold within a bioreactor is a promising method for engineering bone tissue external to the body. We propose a mathematical model, and employ a suite of candidate constitutive laws, to qualitatively describe the effect of applied hydrostatic pressure on the quantity of minerals deposited in such an experimental setup. By comparing data from numerical simulations with experimental observations under a number of stimulation protocols, we suggest that the response of bone cells to an applied pressure requires consideration of two components; i) a component describing the cell memory of the applied stimulation, and ii) a recovery component, capturing the time cells require to recover from high rates of mineralisation.

**Keywords:** Modelling, Tissue engineering, Ordinary differential equation, Biomechanical response

---

## 1. Introduction

*In vitro* tissue engineering is a method for creating functional tissue and organ samples external to the body, with the aim of replacing damaged or diseased tissues and organs (Rose and Oreffo, 2002; Martin, 2004). Our particular focus is on bone tissue engineering. By using autologous cells (donor and recipient being the same person), often seeded onto or into a scaffold which acts as a template for the developing tissue, tissue engineered products have many advantages for the replacement or treatment of damaged or diseased bone over traditional approaches, such as either bone grafting or non-living prostheses. The quantity of autologous bone that can be harvested for a bone graft is limited and the surgical procedures involved have a high risk of complications, while there can be problems with rejection and infection during allogeneic (donor and recipient being different people) bone grafting (Dimitriou et al., 2011; Schroeder and Mosheiff, 2011). Non-living prostheses, for example metallic or ceramic implants, are not able to easily biologically integrate into the surrounding tissue. Moreover, they have different mechanical properties to that of bone that can lead to weakening at the bone-implant interface, and they can require surgical revision after several years of use (Schroeder and Mosheiff, 2011). The engineering of functional bone tissue implants is an alternative strategy to replace bone, and is free from some of these risks and disadvantages. However, to date, only simple avascular tissues have been successfully engineered to a standard appropriate for their use *in vivo* (Orlando et al., 2011; Wong et al., 2010). Research into methods for increasing the quality and quantity of tissue engineered products is essential. This requires a more detailed understanding of the processes involved during tissue development.

The development of the growing tissue construct, a term used to describe the combination of scaffold, cells, extracellular matrix and fluid, often occurs within a bioreactor. The use of a bioreactor enables

---

\*Corresponding author

Email addresses: leonard@itwm.fraunhofer.de (K.H.L. Neßler), j.r.henstock@liverpool.ac.uk (J.R. Henstock), a.j.el.haj@keele.ac.uk (A.J. El Haj), waters@maths.ox.ac.uk (S.L. Waters), jonathan.whiteley@cs.ox.ac.uk (J.P. Whiteley), jmosborne@unimelb.edu.au (J.M. Osborne)

Preprint submitted to JTB

December 5, 2015

precise control of the biophysical and biochemical environment experienced by the construct during growth (Rauh et al., 2011; El Haj and Cartmell, 2010; Yeatts and Fisher, 2011). Cells respond to both biomechanical and biochemical cues and thus need to be subjected to the correct mechanical and biochemical environment to function appropriately (El Haj et al., 2005). This is particularly important in the development of mechanosensitive tissues, such as bone (Mullender et al., 2004).

Bone tissue consists of three main components: mineralised bone matrix, cells and interstitial fluid. The mineralised bone matrix consists of an organic matrix along with solid inorganic mineral, mostly in the form of hydroxyapatite (Buck and Dumanian, 2012). The process of mineralisation of the matrix involves the conversion of soluble inorganic ions, dissolved in the bone fluid, into solid apatite crystals deposited on the collagen to form a composite which gives bone its ability to withstand loading forces (Clarke, 2008).

Within the body, bone tissue growth and regulation is coordinated by three main cell types: osteoblasts, osteoclasts and osteocytes. Osteoblasts secrete large amounts of specialised extracellular matrix known as osteoid, composed largely of type I collagen. As the cells and the matrix both mature, the secreted proteome changes to include molecules with adaptations for mineralising and structurally modifying the matrix, including alkaline phosphatase, osteocalcin, osteopontin and osteonectin (Gorski, 2011). The presence of these proteins in the extracellular matrix promotes the crystallisation of calcium and phosphate in the interstitial fluid into a basic form of hydroxyapatite aligned with the collagen fibrils, resulting in it becoming increasingly ossified, a process often termed primary mineralisation (Buehler, 2007; Boivin, 2007). Secondary mineralisation occurs over a longer period of time, between several months to years, in order to strengthen the bone with more resilient matrix and is associated with changes in both the crystalline composition of the bone and the composition of proteins in the extracellular matrix (Henstock et al., 2015; Fuchs et al., 2008; Bala et al., 2010). Osteoclasts degrade existing mineralised bone matrix, while osteocytes are a highly specialised cell type and are the main mechanosensors within bone tissue, converting mechanical signals into the biochemical cues to which osteoblasts and osteoclasts then respond, and hence regulate the local microstructure of the skeleton (Mullender et al., 2004). Osteoblasts arise from mesenchymal stem cells through differentiation, and can further mature into osteocytes, whereas osteoclasts arise from a separate cell lineage, and are differentiated from haematopoietic stem cells (Buck and Dumanian, 2012). Mechanical stimulation is essential for the maintenance and health of bone tissue, and the coordination of the functions of these different cell types (Chen et al., 2010; Liu et al., 2010; El Haj et al., 2005), although the precise cellular response to mechanical loading is still unknown and is an active area of research.

The mathematical model developed in this paper is based on an experimental setup consisting of a mixture of active osteoblasts and osteocytes. Although osteoblasts use certain digestive enzymes to migrate through their environment and remodel their surrounding extracellular matrix, they are generally considered to be tissue-forming, rather than degrading cells (Paiva and Granjeiro, 2014). Therefore, we determine that the main phenomena that we are investigating is that of primary mineralisation, and subsequent changes in the secondary phase of mineralisation are expected to have a very limited input due to the short duration and lack of osteoclasts in the experiment.

Mathematical modelling, in conjunction with biological experiments, has an important role to play in elucidating biological mechanisms occurring during the growth and development of tissues, and providing information that cannot be experimentally measured. Once a mathematical model is validated, it may be used to optimise the experimental strategy, with the aim of improving the quality of tissue engineered products. Several theoretical models have been developed to describe the growth of engineered tissues, as reviewed in O’Dea et al. (2012). However, to the authors’ knowledge, no mathematical models have been developed to describe the response of bone-producing cells to hydrostatic pressure stimulation. We note that a series of related papers adopted a multiphase modelling approach to investigate the effect of the pressures generated due to fluid motion and tissue growth within a perfusion bioreactor on the tissue composition, upon which the first of our models is loosely based (O’Dea et al., 2008, 2010; Osborne et al., 2010), although a comparison to experimental data was not made. It should be noted that a number of hypotheses exist for predicting the formation of different tissue types (for example, bone, cartilage and connective tissue) under different mechanical stimulation protocols and magnitudes *in vivo*. Recent reviews of mathematical models based on these hypotheses may be found in Isaksson (2012) and Boccaccio et al. (2011). It is an open question whether the hypotheses proposed are valid for *in vitro* tissue engineering studies (Khayyeri et al., 2009). However, we note that a number of these studies have hypothesised that bone mineralisation is affected by memory of the loading protocol. For example Levenston et al. (1994) included a fading memory component in their model of bone adaptation

in response to mechanical loading *in vitro*, although no direct comparison to experimental data was made.

We develop a suite of mathematical models to elucidate the role of applied hydrostatic pressure on the quantity of minerals deposited in the engineering of a bone construct. It is well documented that hydrostatic pressure stimulation promotes stem cell differentiation down the chondrogenic lineage to form cartilaginous tissues (Elder and Athanasiou, 2009). In contrast, the effects of hydrostatic pressure on bone cells, and the resultant effect on the bone tissue composition, has received less attention and is not well understood (Chen et al., 2010; Liu et al., 2010; Hess et al., 2010). It is known that hydrostatic pressure is experienced by cells residing in the marrow space (Chen et al., 2010), and the physiological pressure within the lacunar–canalicular system has been estimated computationally to reach 274 kPa during a typical walking loading strategy, with higher pressures being obtained during impact loading (Zhang et al., 1998b,a). When artificially engineering bone in a bioreactor, cyclical or dynamic pressure is typically applied because it is physiologically more realistic than a constant applied pressure, and has been shown to produce constructs with more of an osteogenic phenotype (a denser and more mineralised construct) (Basso and Heersche, 2002; Roelofsen et al., 1995). A variety of experimental studies on the effects of hydrostatic pressure on bone tissue development have been performed, using a range of cell types. Results indicate that dynamic hydrostatic pressure has a positive influence on bone development; it has been shown that hydrostatic pressure stimulation causes increased intracellular concentration of calcium ions (Liu et al., 2010), increased matrix mineralisation (Roelofsen et al., 1995) increased collagen and calcium content (Nagatomi et al., 2003), decreased levels of osteocyte cell apoptosis (Liu et al., 2010), increased osteocyte viability (Takai et al., 2004), and ultimately increased bone growth and mineralization (Henstock et al., 2013).

We now detail the experiments on which we base our hypotheses, leading to the development of our mathematical models.

### 1.1. Experimental observations

Our focus here is on *qualitatively* representing an *in vitro* experimental setup of a mixture of active osteoblasts and osteocytes seeded in a collagen gel and submerged in a culture medium. The culture media contains nutrients, growth hormones and mineral ions, and is refreshed on a daily basis. The samples are subjected to sessions of hydrostatic pressure loading with the aim of testing the hypothesis that cyclic hydrostatic pressure stimulation results in a higher volume of minerals than in the absence of loading. The hydrostatic pressure bioreactor comprises a sealed vessel and a machine capable of compressing incubated air above a 6-well plate. Computer controlled compression of the gas phase allows for precise regulation of the frequency and amplitude of the pressure applied. Further details on the bioreactor equipment may be found in Henstock et al. (2013). Three separate loading strategies are considered:

**Oscillatory loading** samples are placed in the bioreactor for one hour per day and subjected to sinusoidal pressure loading with a given amplitude and frequency, with the remaining time spent at atmospheric pressure;

**Constant loading** samples are placed in the bioreactor for one hour per day and subjected to a constant given pressure, with the remaining time spent at atmospheric pressure;

**Control loading** samples remain at constant atmospheric pressure for the entire experiment.

The experimental method of quantifying changes in the mineral volume of the constructs is by direct measurement of the construct by X-ray microtomography ( $\mu$ CT) and subsequent segmentation analysis. Each individual voxel of the  $\mu$ CT image has a related X-ray opacity (intensity), which is directly equivalent to the amount of calcification (referred to as bone mineral density, BMD, in most medical applications), where the voxel size is determined by the resolution of the scanner. The mineralised volume is defined as the number of voxels of the material above a certain defined threshold. As the quantity of deposited minerals increases, more voxels will come within the pre-determined density threshold and be counted as “mineralised”, resulting in both the measured mineralised volume and the average density of the images increasing.

Preliminary runs of the cell-seeded collagen gel experiments, which we wish to model, illustrated the same trends as those presented in Henstock et al. (2013), which examined the bone density and volume of mineralisation of femurs, removed from 11 day old chick foetuses. The main experimental observations, which motivate our models, are as follows:

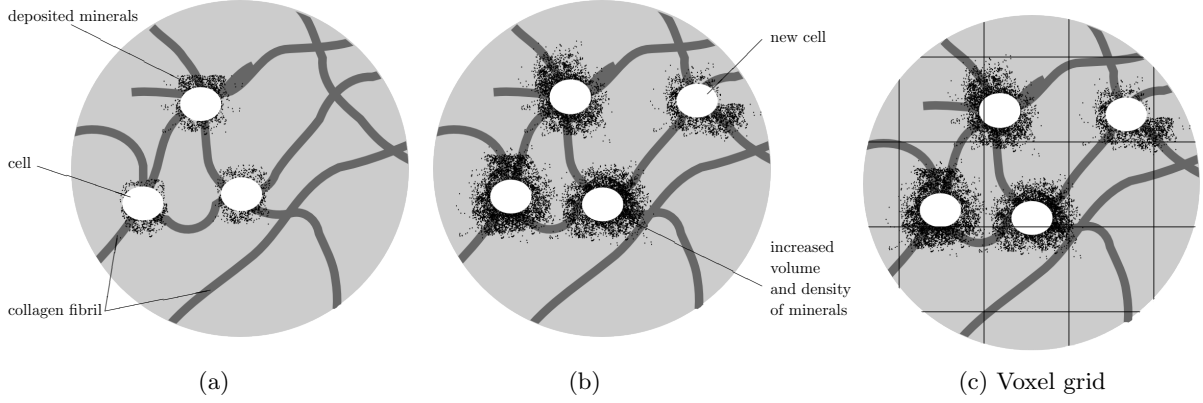


Figure 1: Schematic to illustrate a 2D cross-section of a portion of the experimental setup we wish to represent. The dark grey material represents the collagen fibrils, with the white circles indicating cells and the black substance illustrating deposited minerals. The light grey background indicates fluid. Figure (b) illustrates (a) at a later timepoint, where there is an increased volume and density of deposited minerals, while (c) indicates the  $\mu$ CT voxel grid. Schematic is not to scale.

**Observation 1 :** samples under oscillatory loading showed a higher mineralised volume and a higher average  $\mu$ CT image density than samples under control loading. In comparison, the mineralised volume and average  $\mu$ CT image density of the samples were the same under constant loading (with a pressure of 279 kPa imposed in the bioreactor) and control loading conditions;

**Observation 2 :** after 14 days, there was a higher volume of mineralisation for samples subjected to oscillatory loading varying between 0 – 279 kPa than samples subjected to oscillatory loading varying between 0 – 7 kPa for fixed frequency;

**Observation 3 :** the average density of the  $\mu$ CT images of the samples was higher under oscillatory loading varying between 0 – 279 kPa with a frequency of 2 Hz than a frequency of 0.005 Hz.

The authors concluded that dynamic variation of the applied pressure is required for an increased quantity of bone production, with the frequency and amplitude of the loading having an effect on the degree of mineralisation.

### 1.2. Mathematical modelling of the effect of hydrostatic pressure on mineralisation rate

In this paper we present a new ordinary differential equation (ODE) model to describe the growth and mineralisation of a collagen gel seeded with a mixture of osteoblasts and osteocytes under hydrostatic pressure loading. As the bone cell response to hydrostatic pressure stimulation is unknown, we examine three candidate mechanisms to describe this response with the aim of qualitatively reproducing the experimental observations detailed in Section 1.1. The available observations, being non-spatial, motivates the use of time dependent ODEs rather than a spatial model.

Experimental results indicate that the volume of collagen remains roughly constant throughout the experimental timeframe. This indicates that the osteoblast cells mainly deposit mineral crystals onto the existing collagen scaffold, rather than additionally secreting extracellular matrix, as indicated in the 2D schematic of the experimental setup in Figure 1. Motivated by this, we model the temporal change in mineral volume, and assume that there is an adequate supply of mineral ions in the fluid, due to the regular renewal of the culture medium, which the osteoblasts can convert into solid minerals on top of the collagen. We make the assumption that the ratio of the number, and consequently volume, of the two cell types in the experimental system, osteoblasts and osteocytes, remains constant throughout the experimental timeframe, enabling us to represent all the cells by a single population. As osteoclasts, which arise from a different cell lineage, are not present in the experimental setup we do not include the effects of mineral degradation.

The dependence of the system on the applied hydrostatic pressure is captured through a pressure-dependent mineralisation rate, and we examine three separate hypotheses for the response of cells to pressure, considering a sequential introduction of physical phenomena. The first hypothesis assumes that cells respond to higher pressures (within physiological ranges) by increasing the rate at which they deposit minerals. In the second model we hypothesise that the length of time at which cells can deposit at

this increased rate is limited, while the third hypothesis makes the assumption that cells require a period of recovery in between each session of depositing minerals at the highest rate. Further mathematical details are given in Section 2 when the models are presented. Numerical simulations for the three separate models are presented in Section 3, and we make a qualitative comparison to the experimental observations described in Section 1.1. To do this, we compare the volume of minerals predicted by our mathematical model to the mineralised volume as measured through imaging techniques in the experiments. This comparison enables us to identify which of the models is the most appropriate in representing the experimental observations detailed in Section 1.1. Finally, we conclude and discuss our results in Section 4.

## 2. Model development

We now present the mathematical model describing the evolution of the volume of cells, represented by  $c(t)$ , and the volume of minerals, represented by  $m(t)$ , through time,  $t \geq 0$ . Our aim is to qualitatively represent the experimental observations, and we present the model in dimensionless variables to allow candidate constitutive laws to be tested. We note that the model developed here is phenomenological in nature however all aspects of the model are motivated by the experimental system. Assuming that the collagen volume of each construct remains constant in time, and that cells need to be attached to the collagen matrix to proliferate (Schwartz and Assoian, 2001; McCoy and O'Brien, 2010), the volume of cells is described by

$$\frac{dc}{dt} = k_b c \left( 1 - \frac{c+m}{r} \right) - k_d c, \quad (1)$$

where  $k_b \geq 0$  is the cell birth rate and  $k_d \geq 0$  is the rate of cell death. In Equation (1),  $r$  represents the maximal volume of the construct that can be occupied by cells, minerals and extracellular fluid. (i.e. total volume of the construct less the volume of collagen, which is constant in time). Here the equations have been non-dimensionalised by this constant volume of collagen within the construct. We choose this particular non-dimensionalisation to allow for the case where the total volume of the construct can change over time, for example when considering the system for longer timescales. However, here we consider this volume to be constant in time. The first term on the right hand side of (1) is a logistic cell birth term that models the effect of the depletion of resources such as fluid and nutrients on the production of new cells. As hydrostatic pressure has not been reported to significantly influence the proliferation rate of bone cells, we make the assumption that the cellular proliferation rate is pressure-independent. The second term on the right hand side of (1) represents cell death, where we ignore the effects of pressure-dependent apoptosis which is witnessed only at very high pressures (Rivalain et al., 2010), orders of magnitude above those found within the bioreactor.

We assume that changes in the volume of minerals through time are attributable to mineral deposition by the osteoblast cells, which gives

$$\frac{dm}{dt} = k_p(t, p(t)) c \left( 1 - \frac{c+m}{r} \right), \quad (2)$$

where  $k_p(t, p(t)) \geq 0$  is the pressure-dependent rate of mineral deposition and  $p(t)$  is the pressure experienced by the cells. As cells are required for mineral deposition to occur (both osteoblasts which deposit the minerals and osteocytes which sense the mechanical stimulation and coordinate the osteoblast response), the rate of increase in minerals is proportional to the cell volume,  $c$ . In addition, as the process of mineralisation requires a supply of mineral ions, the rate of mineralisation is also dependent on the volume fraction of fluid, represented by the term  $(1 - (c+m)/r)$  in a similar manner to that in (1). As for the cell birth term in (1) we require that  $c(t) + m(t) \leq r$  holds so that the mineralisation term in (2) is non-negative. In fact due to the structure of the equations if  $c(0) + m(0) \leq r$  then  $c(t) + m(t) \leq r$  holds for all times  $t$ , which we now show. If  $c(t) + m(t) = r$  for a particular  $t$ , then by summation of (1) and (2), we have  $\frac{d}{dt}(c+m) = -ck_d \leq 0$ . Therefore, the joint volume of cells and minerals cannot increase and thus  $c(t) + m(t) \leq r$  is maintained. Consequently, given  $c(0) + m(0) \leq r$  then  $c(t) + m(t) \leq r$  is always satisfied. Furthermore if we enforce the physically realistic conditions  $c(0) \geq 0$  and  $m(0) \geq 0$  then using  $c(t) + m(t) \leq r$  and Equation (1) we see that  $c(t) \geq 0$  for all  $t$ . Similarly Equation (2) enforces  $m(t) \geq 0$  for all  $t$ . Therefore  $0 \leq c(t), m(t) \leq r$  for all  $t$ .

We assume that the pressure,  $p(t)$ , is equal to that exerted on the surface of the culture medium. To represent the loading strategies investigated experimentally, we set

$$p(t) = \begin{cases} f(t), & \text{if the construct is in the bioreactor,} \\ 0, & \text{otherwise,} \end{cases} \quad (3)$$

where  $f(t)$  describes the form of the applied pressure loading and a zero dimensionless pressure corresponds to atmospheric pressure. The loading strategies employed in Henstock et al. (2013) are described by

$$f(t) = \begin{cases} a(1 - \cos(2\pi\omega t)), & \text{for oscillatory pressure loading,} \\ 2a, & \text{for constant pressure loading,} \end{cases} \quad (4)$$

where  $a$  and  $\omega$  are constants that describe the amplitude and frequency of the applied loading experienced within the bioreactor and  $0 \leq p \leq 2a$ . Initial conditions for (1) and (2) are given by prescribed values of  $c(0)$  and  $m(0)$ . Recalling that  $r$  is the maximum total volume of cells and minerals, we assume that  $c(0) + m(0) \leq r$ .

To close the system of equations given by (1) – (4) we require a description of the pressure-dependent mineral deposition rate  $k_p$ . We now postulate three candidate constitutive laws for  $k_p$  and examine the predicted response of the system. We then make qualitative comparisons with the experimental observations discussed in Section 1.1, allowing us to gain insights into the nature of the bone cell response to hydrostatic pressure loading.

### 2.1. Modelling the cell response to pressure

We now introduce and compare three separate models for  $k_p$ , incorporating additional physical phenomena in turn, as follows.

#### 2.1.1. Model 1

The experimental observations in Section 1.1 indicate that there exists a range of pressures to which bone cells respond by converting more minerals from ions in solution into solids (observation 2). Motivated by this, we assume that the rate of mineralisation is enhanced when the applied pressure is above a threshold,  $p_1$ , in comparison to pressures below the threshold,  $p < p_1$ , and represent this mathematically by

$$k_p(t, p(t)) = \begin{cases} k_2, & \text{if } p(t) \geq p_1, \\ k_1 & \text{if } p(t) < p_1, \end{cases} \quad (5)$$

where  $k_2 > k_1 > 0$ . We note that this model resembles that used by O’Dea et al. (2008, 2010) and Osborne et al. (2010), based on the experimental findings of Roelofsen et al. (1995), with the exception that we here do not include a higher threshold above which mineralisation ceases. Although experimental findings suggest that very high pressures (above 100 – 200 MPa) are inhibitory (Rivalain et al., 2010), the experiments performed to date have not included such high pressures. The possibility of modifying the model in (5) to encompass the response under significantly higher applied pressures is discussed in Section 4.

#### 2.1.2. Model 2

The experiments described in Section 1.1 indicate that dynamic stimulation is needed to develop an osteogenic phenotype, with constant applications of higher pressure resulting in less mineral deposition than oscillatory loading (observation 1). Motivated by this, we now hypothesise the presence of signalling molecules, released by the cells when pressure exceeds the threshold,  $p_1$ , that are required for cells to deposit minerals at the higher rate of  $k_2$ . Assuming there are limited supplies of these molecules, which are regenerated instantly when the pressure drops below  $p_1$ , we assume that cells may only deposit minerals at a rate of  $k_2$  for a total time  $T_1 \geq 0$ , before returning to deposit at a rate  $k_1$ . We note that the signalling pathways controlling the response to biomechanical loading are highly regulated and complex (Mullender et al., 2004; Klein-Nulend et al., 2005; Chen et al., 2010; Rawlinson et al., 1991), but this model aims to represent the cascade of cell signalling processes that occur during and after the

application of loading. Denoting the last time that the mineralisation rate increased from  $k_1$  to  $k_2$  by  $t_1(t)$ , the rate of mineral deposition is described by

$$k_p(t, p(t)) = \begin{cases} k_2, & \text{if } p(t) \geq p_1 \text{ and } t - t_1(t) \leq T_1, \\ k_1, & \text{otherwise.} \end{cases} \quad (6)$$

We need to prescribe an initial value for  $t_1$ , so that the model is well-defined for cases where the applied pressure is above the pressure threshold at the initial timepoint, i.e.  $p(0) \geq p_1$ . We set  $t_1(0) = 0$ , so that if the pressure is initially above  $p_1$ , the cells can begin to deposit minerals at the rate  $k_2$  at  $t = 0$ .

### 2.1.3. Model 3

The form for  $k_p(t, p(t))$  given in (6) implies that the stores of signalling molecules are instantly regenerated when the pressure drops below the threshold. This assumption may not be sufficiently accurate when the frequency of the applied cyclic loading is so high that cells cannot sense and respond to changes in applied pressure. To account for the time required to regenerate the stores of these molecules, we further modify Model 2 by hypothesising that cells require a total time  $T_2 \geq 0$  at pressures below the threshold to regenerate the stores of the signalling molecules before deposition at the higher rate of  $k_2$  can occur again. We denote the last time that the mineralisation rate decreased from  $k_2$  to  $k_1$  by  $t_2$ , and define the indicator function  $\chi$  by

$$\chi(t) = \begin{cases} 1, & \text{if } p(t) < p_1, \\ 0, & \text{if } p(t) \geq p_1, \end{cases} \quad (7)$$

so that the quantity  $\int_{t_2(t)}^t \chi(\tau) d\tau$  represents, at time  $t$ , the total time since  $t_2$  (the time that the applied pressure has satisfied  $p < p_1$ ), and consequently the regeneration time elapsed. We note that another modelling approach could have been to consider recovery as occurring when  $k_p \neq k_2$ , and so when cells are not mineralising the collagen at the higher rate. However, we here make the hypothesis that the pathways controlling the cellular response of mineralisation remain saturated, for example through blocked ion channels, until the applied pressure drops below the pressure threshold which then has the effect of opening these pathways. Such a hypothesis is motivated by previous work demonstrating that a rest in between loading applications is required for optimal osteocyte signalling due to the time required to regenerate resources (Ausk et al., 2004). Using this hypothesis we now define  $k_p(t, p(t))$  as

$$k_p(t, p(t)) = \begin{cases} k_2, & \text{if } p(t) \geq p_1 \text{ and } t - t_1(t) \leq T_1 \text{ and } \int_{t_2(t)}^t \chi(\tau) d\tau \geq T_2, \\ k_1, & \text{otherwise.} \end{cases} \quad (8)$$

We are required to provide an initial value of  $t_2$ . Setting  $t_2(0) = -T_2$  means that cells can start depositing the first time the pressure goes above  $k_2$ , which is appropriate as prior to this cells have been resting.

## 2.2. An overview of the three models

We now demonstrate the form of  $k_p(t, p(t))$  for Models 1 – 3 when the system is subject to an applied cyclic pressure loading regime which oscillates between pressures of 0 and  $2a$ . Illustrative parameters,  $T_1 = 1/5\omega$ ,  $T_2 = 3/5\omega$ ,  $k_2 = 10k_1$  and  $p_1 = 8a/7$ , are used and the forms of  $k_p(t, p(t))$  are shown in Figure 2. The response of all three models under a static application of applied pressure above the pressure threshold is shown in Figure 3.

Under an oscillatory loading strategy, the time the applied pressure is above the pressure threshold each cycle of loading is given by

$$\tau = \begin{cases} \frac{1}{\pi\omega} \left( \pi - \arccos \left( 1 - \frac{p_1}{a} \right) \right), & \text{if } 2a \geq p_1, \\ 0, & \text{if } 2a < p_1, \end{cases} \quad (9)$$

and this is illustrated in Figure 2.

Model 1 allows cells to perform mineralisation at a rate  $k_2$  when pressures are above the pressure threshold  $p_1$ , see Figure 2(a). In this case, the length of time cells deposit minerals at a rate  $k_2$  each

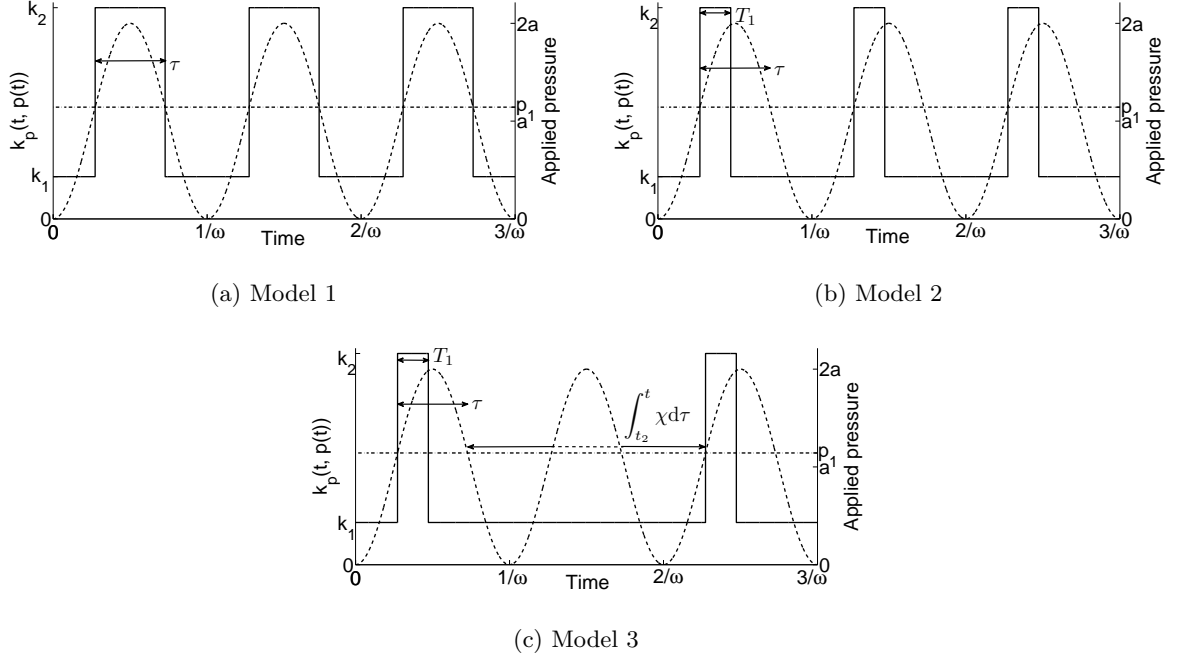


Figure 2: Illustration of the difference between the three models of the mineralisation rate, given by (5), (6) and (8), with parameters chosen for illustrative purposes. The solid black line indicates the mineral deposition rate in response to the cyclic applied pressure above atmospheric pressure, illustrated by the dashed black line. The horizontal dot-dashed lines indicate the position of the pressure threshold,  $p_1$ . The total amount of time,  $\tau$ , that  $p \geq p_1$  for each cycle of loading as given by (9), is shown. The quantity  $T_1$ , the total time at which cells can deposit at the rate  $k_2$ , is indicated on Figures (b) – (c). The integral  $\int_{t_2(t)}^t \chi(\tau) d\tau$ , describing the total recovery time, is indicated in (c), where the dotted portion does not contribute to the integral as  $p > p_1$  during this time period.

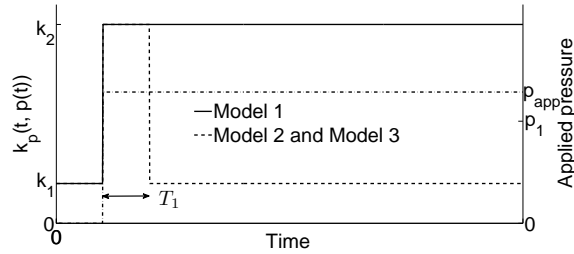


Figure 3: The response of the three separate models for the mineralisation rate to a constant application of higher pressure loading,  $p_{app}$ , where  $p_{app} \geq p_1$ . The dot-dashed line shows the applied pressure, while the solid black line shows the mineralisation rate for Model 1 and the dashed black line shows the mineralisation rate for both Models 2 and 3, which are identical assuming cells have rested sufficiently before the application of  $p_{app}$ .



cycle of oscillatory loading is always equal to  $\tau$ . In the case of a static application of an applied pressure lying above the pressure threshold, the model states that cells remain depositing minerals at the higher rate, see Figure 3.

Model 2 limits the total of time the cells can deposit at the higher rate, see Figure 2(b). Now cells cease depositing at a rate  $k_2$  while the pressure is still above the pressure threshold, as  $T_1 < \tau$  for the illustrative parameters chosen. In the case of a static application of an applied pressure above the pressure threshold, this model predicts that the cells deposit at the higher rate of  $k_2$  for a time of  $T_1$  after which they would deposit at a rate  $k_1$  for the remainder of the time, see Figure 3.

The third model takes account of the time needed for the regeneration of the stores of the signalling molecules to occur, see Figure 2(c); here the time below the threshold in between each loading cycle is insufficient for these stores to be regenerated, and so mineralisation at the higher rate occurs every other cycle.

We note that Model 1 may be considered a subset of Model 2, which may, in turn, be considered a subset of Model 3. As  $T_1$  approaches infinity (or the length of the experiment), Model 2 becomes identical to Model 1, as  $t - t_1(t) \leq T_1$  is always satisfied. This is equivalent to cells having sufficient stores of signalling molecules to allow them to mineralise uninterrupted for an infinite length of time (or a time equal to the length of the total experiment). When  $T_2 = 0$ , Model 3 is identical to Model 2, as regeneration of the signalling molecules stores occurs the instant the pressure drops below the pressure threshold and the inequality  $\int_{t_2(t)}^t \chi(\tau) d\tau \geq T_2$  always holds.

### 3. Model predictions

Inspired by the experiments described in Section 1.1 we consider three separate loading strategies, and compare the predictions by Models 1 – 3 for the quantity of minerals deposited. The first loading strategy, *oscillatory stimulation* loading, models samples placed in the bioreactor for 1 time unit every 24 time units, under cyclic loading at an amplitude of  $a$  pressure units and frequency of 3600 per unit time, and otherwise experiencing atmospheric pressure. The second loading strategy, *constant stimulation* loading, models samples that are also placed in the bioreactor for 1 time unit every 24, during which time they experience a constant pressure of  $2a$ . The final loading strategy, the *control* loading strategy, models samples that remain outside the bioreactor for the total duration of the experiment, where they experience atmospheric pressure. We restrict  $\omega$  to non-negative integer values, so that each session in the bioreactor consists of an integer number of full cycles of loading.

Parameters are chosen to illustrate the range of possible behaviours of the system. We set  $p_1 = a = 1$  and  $r = 1$ . We set the initial conditions to be  $c(0) = 0.2$  and  $m(0) = 0$ . Setting  $\omega = 3600$  (equivalent to 1 Hz if one time unit is equal to one hour), we choose  $T_1$  to be the same order of magnitude as the time that the applied pressure is above the threshold  $p_1$  during each cycle of the oscillatory stimulation loading regime, and  $T_2$  is chosen to be slightly smaller than this. The choice of the remainder of the parameters is motivated by those obtained through comparison of a similar model to preliminary experiments in Leonard (2014). These parameters are given in Table 1.

Table 1: Default dimensionless parameters for the numerical simulation.

$k_b$	$=$	$24^{-1}$	$k_d$	$=$	$2.5 \times 10^{-4}$
$k_1$	$=$	$2.5 \times 10^{-2}$	$k_2$	$=$	5.0
$r$	$=$	1.0	$p_1$	$=$	1
$T_1$	$=$	$10^{-4}$	$T_2$	$=$	$7 \times 10^{-5}$
$\omega$	$=$	3600	$a$	$=$	1

#### 3.1. Rates of construct mineralisation

Figure 4 compares the mineral volume predicted by Models 1 – 3 under the three loading strategies, using the parameters given in Table 1. The volume of minerals predicted by Models 1 – 3 at the experimental end point (480 units of time) under the three loading conditions is summarised in Table 2.

We see in Figure 4(a) that Model 1 predicts that mineral deposition is highest under the constant stimulation loading strategy, with the oscillatory loading strategy showing less mineral volume by the experimental end point. According to Model 1, cells can deposit at the higher rate of  $k_2$  for the whole

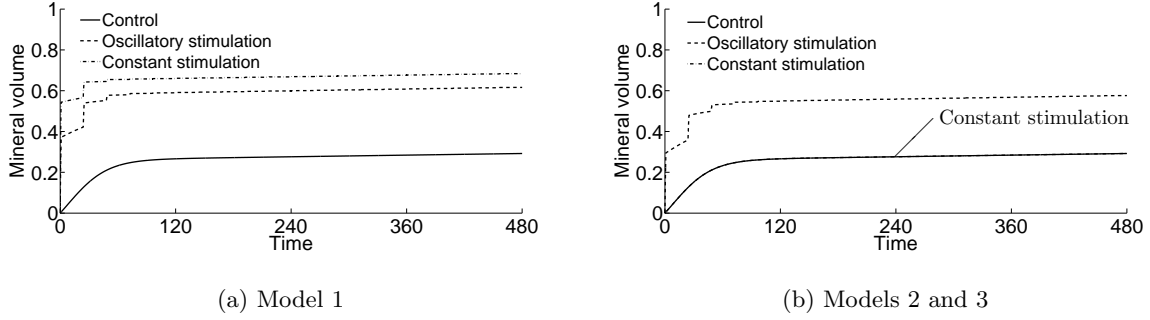


Figure 4: Predicted mineralised volume under the three different loading regimes, for the three different models of mineral deposition used, with dimensionless parameters set as in Table 1. In (b), the lines representing the control and constant stimulation loading regimes are visually indistinguishable.

duration of the time they are in the bioreactor under the constant stimulated loading strategy. Under the oscillatory loading strategy, cells may deposit at the higher rate of  $k_2$  only for a portion of this time, as the applied pressure is above the pressure threshold intermittently, and hence there is less mineral deposition overall. For the control loading conditions the applied pressure is always below the threshold  $p_1$  and so mineral deposition occurs at the lower rate  $k_1$  throughout the experimental time period resulting in the lowest quantity of minerals deposited. The mineral volume predicted under the constant stimulation loading strategy for Model 1, being higher than the volume predicted under the oscillatory stimulation loading strategy, contradicts experimental evidence (observation 1) and previous work, which demonstrates that dynamic rather than static loading is needed to maintain high levels of mineral deposition (Henstock et al., 2013). Hence Model 1 is insufficient to replicate experimental observations for all parameter sets.

Table 2: Mineral volume after 480 time units, with the percentage change above control loading conditions in brackets, to 3 s.f.

Model	Control	Oscillatory Stimulation	Constant Stimulation
1	0.292	0.616 (111 %)	0.684 (134 %)
2	0.292	0.576 (97.2 %)	0.292 (0.06 %)
3	0.292	0.576 (56.2 %)	0.292 (0.06 %)

In contrast to Model 1, both Model 2 and Model 3 predict a similar volume of minerals deposited under the control and the constant stimulated loading strategies, with the intermittent cyclic loading showing a higher volume of minerals deposited over the experimental timeframe, thereby representing the experimental observations 1 and 2. Due to the small size of  $T_2$ , these two models yield identical behaviour under the loading strategies examined for the parameters in Table 1 as  $\int_{t_2(t)}^t \chi(\tau) d\tau \geq T_2$  is always satisfied. According to Models 2 and 3, cells can respond by depositing minerals at the higher rate of  $k_2$  for only a time  $T_1$  under the constant stimulated loading regime while in the bioreactor due to the saturation of the pressure-sensing intracellular mechanisms, after which they resume depositing at the lower rate of  $k_1$ , as indicated in Figure 3. This results in the total mineral volume at the experimental end time point being only marginally higher under the constant stimulation than the control loading regime, see Table 2. Under the intermittent oscillatory loading strategy, the stores of signalling molecules are continually regenerated, allowing cells to deposit at the higher rate of  $k_2$  for a significant portion of the time and resulting in more mineral volume. These results indicate that Models 2 and 3 are more representative of cell response to pressure loading than the first model.

The effect of the recovery time  $T_2$  on the behaviour predicted by Models 2 and 3 is examined in the next section. This difference in the response to applied pressure is then used in Section 3.3 to distinguish between these two models by examining the behaviour they predict under the oscillatory stimulation loading regime for a range of amplitudes and frequencies.

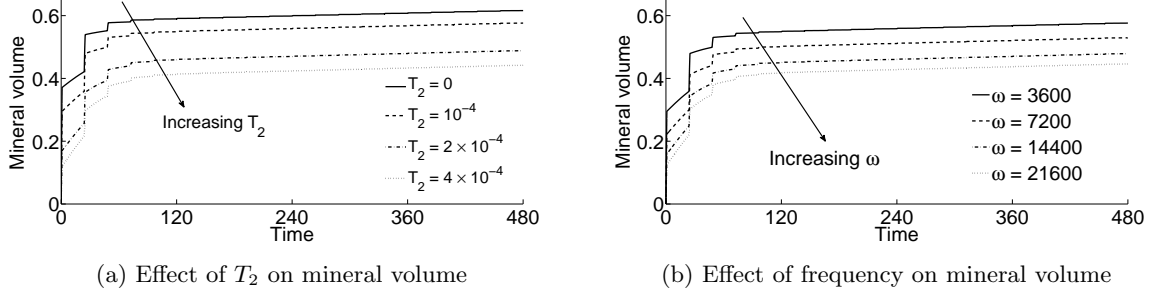


Figure 5: Predicted mineral volume over time under the oscillatory stimulation loading strategy for varying  $T_2$  (Figure 5(a)) and varying frequency (Figure 5(b)), to illustrate the effect the parameter  $T_2$  has on the mineral volume over time. In (a) frequency is fixed at 3600 per unit time and  $T_2$  is varied as shown in the legend. In (b)  $T_2$  is fixed at  $7.0 \times 10^{-5}$  units of time and the frequency of the loading is varied as shown in the legend. All other parameters are given in Table 1.

### 3.2. The effect of the recovery time, $T_2$

Under an oscillatory loading strategy the time that the applied pressure is below the pressure threshold ( $p_1$ ) each cycle is given by  $(1/(\pi\omega))(\arccos(1 - p_1/a))$ . According to Model 3 (defined by Equation (8)) if the integer  $n$  satisfies

$$\frac{n-1}{\pi\omega} \left( \arccos \left( 1 - \frac{p_1}{a} \right) \right) < T_2 \leq \frac{n}{\pi\omega} \left( \arccos \left( 1 - \frac{p_1}{a} \right) \right),$$

then cells require  $n$  cycles of loading ( $n = 1, 2, 3, \dots$ ) to recover from depositing minerals at the higher rate before sufficient stores of the signalling molecules are regenerated to allow mineral deposition at the higher rate to resume. This is equivalent to the forcing frequency satisfying

$$\frac{n-1}{T_2\pi} \left( \arccos \left( 1 - \frac{p_1}{a} \right) \right) < \omega \leq \frac{n}{T_2\pi} \left( \arccos \left( 1 - \frac{p_1}{a} \right) \right). \quad (10)$$

Consequently, the behaviour predicted by Model 2 departs from that of Model 3 when  $n > 1$  and so  $\pi\omega T_2 > \arccos(1 - p_1/a)$ , in which case cells cannot deposit minerals at the higher rate of  $k_2$  each cycle of oscillatory loading, reducing the average rate of mineral deposition and consequently the total quantity by the experimental end point. To illustrate the effect of the parameter  $T_2$ , the mineral volume versus time is plotted in Figure 5(a) for varying  $T_2$ . Model 3 is identical to Model 2 when  $T_2$  is zero, as  $\int_{t_2(t)}^t \chi(\tau) d\tau \geq T_2$  is automatically satisfied. When  $T_2$  is increased to  $10^{-4}$  units of time, Model 3 predicts that cells can only deposit minerals at the higher rate every other cycle of oscillatory loading, so the mineral deposition rate resembles that shown in Figure 2(c). This has the effect of reducing the average mineral deposition rate during the sessions in the bioreactor and, as a consequence, results in less minerals being deposited. As  $T_2$  is increased further, to  $2 \times 10^{-4}$  and  $4 \times 10^{-4}$  units of time, the model predicts that cells can only deposit minerals at the higher rate of  $k_2$  every third and every fourth cycle of the oscillatory loading respectively, resulting in less volume of minerals.

A similar effect is seen as the frequency of oscillatory loading is increased, as illustrated in Figure 5(b). At a frequency of  $\omega = 3600$  cells can deposit at the higher rate each cycle of oscillatory loading. When the frequency is doubled to 7200 per unit time, cells can only deposit every other cycle of loading. At frequencies of 14400 and 21600 per unit time, cells require three and four cycles of loading respectively to regenerate sufficient stores of the signalling molecules after depositing minerals at the higher rate, before they have sufficient stores to deposit at the higher rate again.

### 3.3. Dependence on stimulation

We now use Models 1 – 3 to investigate the predicted volume of minerals deposited under a range of oscillatory stimulation loading regimes, where we consider variations in amplitude (fixed frequency) and then frequency (fixed amplitude) in turn.

#### 3.3.1. The effect of loading amplitude

Figure 6(a) shows the predicted absolute increase in the mineral volume at the experimental end point under oscillatory stimulation compared to the control loading conditions, for varying amplitude

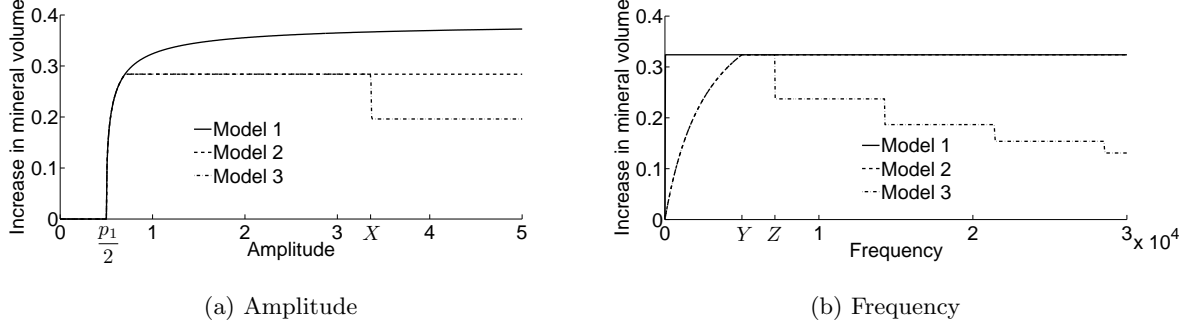


Figure 6: Predicted absolute increase in the mineral volume under oscillatory stimulation over control loading conditions, for varying amplitude and fixed frequency at 3600 per unit time in (a), and varying frequency with fixed amplitude at 1 in (b). The lines for Models 2 and 3, for frequencies below 5000, and the lines for Models 1 and 2 for frequencies above 5000 per unit time, are indistinguishable in (b). Remaining parameters are given in Table 1. The  $X$  in (a) and the  $Z$  in (b) indicate where the results from Models 2 and 3 deviate, at an amplitude of 3.36 pressure units and a frequency of 7143 per unit time respectively. The  $Y$  in (b) indicates where  $\tau = T_1$ , which occurs at a frequency of 5000 per unit time.

with frequency fixed at 3600 per unit time. All models show a zero increase in mineral volume when  $a < p_1/2$ , as the applied pressure never exceeds the threshold  $p_1$  and consequently cells deposit minerals at a constant rate of  $k_1$  under both loading regimes for all models. As the amplitude increases and  $a \geq p_1/2$ , the volume of minerals deposited under the oscillatory stimulation over the control loading regime increases, as the applied pressure is above the pressure threshold for more time, resulting in cells depositing minerals at the rate  $k_2$  for longer. This increase ceases for Models 2 and 3 when the amplitude is sufficiently high that the total time the applied pressure is above the pressure threshold each cycle of loading,  $\tau$ , is greater than  $T_1$ , i.e.  $\tau > T_1$ . In this case, as the amplitude increases further, the total time cells can deposit at the higher rate of  $k_2$  remains fixed at  $T_1$  each cycle of loading, and so the graph exhibits a plateau. Model 1 does not include this limitation, and so the volume of minerals deposited under oscillatory stimulation over the control loading conditions continues to increase. By Equation (10), the quantity of minerals predicted by Model 2 differs from that of Model 3 when  $a > p_1/(1 - \cos(\pi\omega T_2))$ . When this occurs, Model 3 predicts cells can no longer deposit minerals at the higher rate every cycle of oscillatory loading, resulting in a decrease in the volume of minerals deposited. For the parameters given in Table 1 this occurs when the amplitude of loading exceeds 3.36 units of pressure, as indicated in Figure 6(a) by an  $X$  on the horizontal axis.

### 3.3.2. The effect of loading frequency

We now turn our attention to investigating the effect of frequency on the increase in mineral volume. Model 1 shows no change in the predicted volume of minerals deposited under the oscillatory stimulation over the control loading conditions as frequency increases for  $\omega > 0$ , as can be seen in Figure 6(b). This is because the portion of time the applied pressure is above the threshold while the sample is in the bioreactor is independent of frequency i.e.  $m\tau$  is independent of  $\omega$ , where  $m$  is the number of cycles of oscillatory loading and is equal to  $\omega$ . This is inconsistent with the results of the experiments described in Section 1.1, which illustrate that the density of the  $\mu$ CT images of the samples, which corresponds to the total volume of minerals, is dependent on the frequency of the cyclic loading regime (observation 3), further demonstrating the inadequacy of Model 1 in representing the physical phenomena under consideration. At low frequencies, the quantity of the signalling molecules limits the length of time cells can deposit minerals at the higher rate of  $k_2$  for Models 2 and 3, as  $\tau > T_1$ . For Models 2 and 3, as the frequency increases,  $\tau$  increases and so the quantity of minerals deposited increases, until the frequency is high enough that  $\tau = T_1$ , which occurs when  $\omega = 5000$  units of time as indicated by a  $Y$  in Figure 6(b). At higher frequencies, Model 2 predicts that frequency has no effect on the quantity of minerals deposited for the same reason as for Model 1;  $m\tau$  is independent of  $\omega$ . Although there is no specific research on the effect of applications of hydrostatic pressure to tissue engineered bone samples at high frequencies to the author's knowledge, physiological ranges are normally chosen for tissue engineering studies, and it is known that adverse effects can occur outside these ranges. As such, experimentally we may expect the cell response to diminish when frequencies become too high for the cells to sense and respond to changes in the applied pressure. Here this is only captured in Model 3, which shows a decreasing quantity of mineral deposited in steps as frequency increases. By Equation (10),  $n$ , the number of cycles of

loading required for cells to recover from depositing minerals at the higher rate, increases with increasing frequency as discussed in Section 3.2 and illustrated by Figure 5(b). This results in a decreased average mineral deposition rate when the frequency of the applied loading is a multiple of 7143 (when  $n$  increases by one), and less total volume of minerals.

These results indicate that the third mineral deposition model is the most appropriate to describe the response of bone-producing cells to hydrostatic pressure loading, assuming that high frequencies of hydrostatic pressure loading are inhibitory for cell mineral deposition. This assumption requires further experimental testing, and is discussed further in the next section.

#### 4. Discussion

We have presented a new mathematical model, described by two coupled ordinary differential equations, to characterise tissue engineered bone growth in a hydrostatic pressure bioreactor. The model describes how the volume of cells and minerals vary over time in response to applied hydrostatic pressure. The effects of cell birth, cell death and mineral deposition are accounted for by our mathematical model. The applied loading strategies employed are chosen for their experimental relevance, although our model is sufficiently flexible to allow alternative and more complicated loading strategies to be employed.

Motivated by experimental observations, which illustrate that stimulation under oscillatory hydrostatic pressure results in a construct with a higher mineralised volume than under no stimulation, we hypothesise that bone-producing cells respond to hydrostatic pressure by altering their mineral deposition rate, and postulate functional forms for this pressure-dependence. The predicted response for three separate hypotheses for the pressure-dependent mineral deposition rate, which show a sequential increase in complexity capturing additional physical phenomena, are compared to experimental observations, for illustrative parameter values. It is known that the response of bone-producing cells to mechanical stimulation is highly regulated (Mullender et al., 2004; Klein-Nulend et al., 2005; Chen et al., 2010). Here, we have assumed a simple response to hydrostatic pressure to represent a large number of different signalling pathways that are present within the experimental setup. The first model, which hypothesises that cells respond to applied pressures above a pressure threshold by increasing their mineral deposition rate, overestimates the volume of minerals deposited when the constructs are subjected to long applications of static elevated pressure. The addition of a temporal limitation in the mineral deposition response in Models 2 and 3 prevents this, which is in line with experimental evidence and current theories of cell biology. Here we hypothesise that the length of time that cells may deposit at a higher rate is limited by stores of signalling molecules, which may only be regenerated when the applied pressure drops below the pressure threshold. This demonstrates the need for dynamic stimulation to maintain a high mineral deposition rate, as has been illustrated in experimental studies (Henstock et al., 2013; Turner, 1998; Klein-Nulend et al., 2005). By considering the response over a range of amplitudes and frequencies of intermittent cyclic loading, we illustrate that Model 3 is likely to be more appropriate than Model 2, as it includes a regeneration time, thereby limiting the mineral deposition rate response as the frequency of loading gets high. This is not included in Model 2, which predicts that the quantity of minerals deposited remains at a maximal value, no matter how high the frequency of oscillatory stimulation with a constant amplitude. Although the response of bone-producing cells under applications of oscillatory loading at high frequencies has not been investigated experientially to the authors' knowledge, this is a reasonable assumption given that physiological ranges of loading are known to stimulate higher quantities of mineralised matrix to be deposited than non-physiological ranges.

A number of assumptions have been made during the development of the models presented here. We assumed that the proportion of osteoblasts, the cells which perform mineralisation, and osteocytes, the cells which sense mechanical stimulation and convert this into chemical signals, remains constant throughout time. Future work on evaluating the time-dependent evolution of the cell numbers of the different cell types would enable more accurate models to be built, where the two cell populations are modelled separately and differentiation, and communication, between the cell types is included. In this paper we have focused on the bone-cell response to pressure stimulation within physiological ranges. If the bioreactor equipment is modified in the future to include applications of significantly higher pressures, then it may be appropriate to consider a second pressure threshold, above which the rate of mineralisation decreases, as well as the effect of pressure-dependent apoptosis that is known to begin to occur at ranges of 100 – 200 MPa (Rivalain et al., 2010). In developing the models presented in this paper, we have ignored spatial effects, assumed the system is well nourished and focused on the temporal response to applied pressure. As such we have neglected the effects of nutrient-limited growth and shear-stress

mediated responses, which may also be influential in the quantity of minerals deposited (Martin, 2004; McCoy and O'Brien, 2010; Yeatts and Fisher, 2011; Riddle and Donahue, 2009; Leonard, 2014).

In conclusion, we have presented a simple model to identify the bone-cell response to dynamic hydrostatic pressure loading in a tissue engineering setup. Our work postulates that cells have some memory of the hydrostatic pressure loading they have received, which limits their mineralisation response on static applications of elevated pressure. Furthermore, assuming that high frequencies of applied oscillatory loading are inhibitory, we have illustrated that the inclusion of a recovery time to higher rates of mineral deposition is important in representing the volume of deposited minerals.

## Acknowledgements

KHLN would like to acknowledge the support of the EPSRC through a Systems Biology Doctoral Training Centre studentship (Grant No. EP/G03706X/1) and Fraunhofer ITWM for support through a postdoctoral Fellowship. JMO would like to acknowledge support from the EPSRC and Microsoft Research Cambridge through grant No. EP/I017909/1 ([www.2020science.net](http://www.2020science.net)). JRH and AEH would like to acknowledge the support of the Biotechnology and Biological Sciences Research Council (BBSRC) through grant No. BB/G010560/1 to Keele University.

The data used to generate the figures presented in this manuscript are available publicly at the following location, <http://dx.doi.org/10.5287/bodleian:ht24wj53r>.

## Author contributions

KHLN : Model development, ran numerical experiments, wrote paper, analysed results. JRH : Model development, wrote paper. AJEH : Model development, wrote paper. SLW : Model development, wrote paper, analysed results. JPW : Model development, wrote paper, analysed results. JMO : Model development, wrote paper, analysed results

## References

- B. J. Ausk, T. S. Gross, and S. Srinivasan. Complexity in cellular networks: rest between loading events is required for optimal osteocyte signalling. *50th Annual Meeting of the Orthopaedic Research Society*, 0194, 2004.
- Y. Bala, D. Farlay, D. Delmas, P. P. J. Meunier, and G. Boivin. Time sequence of secondary mineralization and microhardness in cortical and cancellous bone from ewes. *Bone*, 46(4):1204–1212, April 2010. doi: 10.1016/j.bone.2009.11.032.
- N. Basso and J. Heersche. Characteristics of in vitro osteoblastic cell loading models. *Bone*, 30(2):347–351, 2002. doi: 10.1016/s8756-3282(01)00678-0.
- A. Boccaccio, A. Ballini, C. Pappalettere, D. Tullo, S. Cantore, and A. Desiate. Finite element method (FEM), mechanobiology and biomimetic scaffolds in bone tissue engineering. *International journal of biological sciences*, 7(1):112–132, 2011. ISSN 1449-2288. URL <http://www.ncbi.nlm.nih.gov/pmc/articles/PMC3030147/>.
- G. Boivin. The hydroxyapatite crystal: a closer look. *Medicographia*, 29(2):126–32, 2007.
- D. W. Buck and G. A. Dumanian. Bone biology and physiology: Part I. The fundamentals. *Plastic and reconstructive surgery*, 129(6):1314–1320, 2012. doi: 10.1097/prs.0b013e31824eca94.
- M. J. Buehler. Molecular nanomechanics of nascent bone: fibrillar toughening by mineralization. *Nanotechnology*, 18(29):295102+, July 2007. ISSN 0957-4484. doi: 10.1088/0957-4484/18/29/295102. URL <http://dx.doi.org/10.1088/0957-4484/18/29/295102>.
- J. Chen, C. Liu, L. You, and C. A. Simmons. Boning up on Wolff's law: mechanical regulation of the cells that make and maintain bone. *Journal of Biomechanics*, 43(1):108–118, 2010. doi: 10.1016/j.jbiomech.2009.09.016.
- B. Clarke. Normal Bone Anatomy and Physiology. *Clinical Journal of the American Society of Nephrology*, 3(Supplement 3):S131–S139, 2008. doi: 10.2215/cjn.04151206.
- R. Dimitriou, E. Jones, D. McGonagle, and P. Giannoudis. Bone regeneration: current concepts and future directions. *BioMed Central Medicine*, 9(1):66+, May 2011. doi: 10.1186/1741-7015-9-66.
- A. El Haj and S. Cartmell. Bioreactors for bone tissue engineering. *Journal of Engineering in Medicine*, 224(12):1523–1532, 2010. doi: 10.1243/09544119JEIM802.
- A. J. El Haj, M. A. Wood, P. Thomas, and Y. Yang. Controlling cell biomechanics in orthopaedic tissue engineering and repair. *Pathologie-biologie*, 53(10):581–589, 2005.
- B. D. Elder and K. A. Athanasiou. Hydrostatic pressure in articular cartilage tissue engineering: from chondrocytes to tissue regeneration. *Tissue Engineering. Part B, Reviews*, 15(1):43–53, 2009. doi: 10.1089/ten.teb.2008.0435.
- R. K. Fuchs, M. R. Allen, M. E. Ruppel, T. Diab, R. J. Phipps, L. M. Miller, and D. B. Burr. In situ examination of the time-course for secondary mineralization of Haversian bone using synchrotron Fourier transform infrared microspectroscopy. *Matrix Biology*, 27(1):34–41, 2008. doi: 10.1016/j.matbio.2007.07.006.
- J. P. Gorski. Biomineralization of bone: a fresh view of the roles of non-collagenous proteins. *Frontiers in bioscience (Landmark edition)*, 16:2598–2621, 2011. ISSN 1093-4715. URL <http://view.ncbi.nlm.nih.gov/pubmed/21622198>.
- J. R. Henstock, M. Rotherham, J. B. Rose, and A. J. El Haj. Cyclic hydrostatic pressure stimulates enhanced bone development in the foetal chick femur in vitro. *Bone*, 53(2):468–477, 2013. doi: 10.1016/j.bone.2013.01.010.

- J. R. Henstock, L. T. Canham, and S. I. Anderson. Silicon: The evolution of its use in biomaterials. *Acta Biomaterialia*, 11:17–26, January 2015. ISSN 17427061. doi: 10.1016/j.actbio.2014.09.025. URL <http://dx.doi.org/10.1016/j.actbio.2014.09.025>.
- R. Hess, T. Douglas, K. A. Myers, B. Rentsch, C. Rentsch, H. Worch, N. G. Shrive, D. A. Hart, and D. Scharnweber. Hydrostatic pressure stimulation of human mesenchymal stem cells seeded on collagen-based artificial extracellular matrices. *Journal of Biomechanical Engineering*, 132(2):021001+, 2010. doi: 10.1115/1.4000194.
- H. Isaksson. Recent advances in mechanobiological modeling of bone regeneration. *Mechanics Research Communications*, 42:22–31, June 2012. ISSN 00936413. doi: 10.1016/j.mechrescom.2011.11.006. URL <http://dx.doi.org/10.1016/j.mechrescom.2011.11.006>.
- H. Khayyeri, S. Checa, M. Tägil, and P. J. Prendergast. Corroboration of mechanobiological simulations of tissue differentiation in an in vivo bone chamber using a lattice-modeling approach. *J. Orthop. Res.*, 27(12):1659–1666, 2009. doi: 10.1002/jor.20926. URL <http://dx.doi.org/10.1002/jor.20926>.
- J. Klein-Nulend, R. G. Bacabac, and M. G. Mullender. Mechanobiology of bone tissue. *Pathologie-biologie*, 53(10):576–580, 2005. doi: 10.1016/j.patbio.2004.12.005.
- K. H. L. Leonard. *Mathematical and Computational Modelling of Tissue Engineered Bone in a Hydrostatic Bioreactor*. PhD thesis, Computational Biology Research Group, Department of Computer Science, Univeristy of Oxford, 2014.
- M. E. Levenston, G. S. Beaupré, C. R. Jacobs, and D. R. Carter. The role of loading memory in bone adaptation simulations. *Bone*, 15(2):177–186, 1994. ISSN 87563282. doi: 10.1016/8756-3282(94)90705-6. URL [http://dx.doi.org/10.1016/8756-3282\(94\)90705-6](http://dx.doi.org/10.1016/8756-3282(94)90705-6).
- C. Liu, Y. Zhao, W. Y. Cheung, R. Gandhi, L. Wang, and L. You. Effects of cyclic hydraulic pressure on osteocytes. *Bone*, 46(5):1449–1456, 2010. doi: 10.1016/j.bone.2010.02.006.
- I. Martin. The role of bioreactors in tissue engineering. *Trends in Biotechnology*, 22(2):80–86, 2004. doi: 10.1016/j.tibtech.2003.12.001.
- R. J. McCoy and F. J. O’Brien. Influence of shear stress in perfusion bioreactor cultures for the development of three-dimensional bone tissue constructs: a review. *Tissue Engineering. Part B, Reviews*, 16(6):587–601, 2010. doi: 10.1089/ten.teb.2010.0370.
- M. Mullender, A. J. El Haj, Y. Yang, M. A. van Duin, E. H. Burger, and J. Klein-Nulend. Mechanotransduction of bone cells in vitro: mechanobiology of bone tissue. *Medical & biological engineering & computing*, 42(1):14–21, 2004. doi: 10.1007/BF02351006.
- J. Nagatomi, B. P. Arulanandam, D. W. Metzger, A. Meunier, and R. Bizios. Cyclic pressure affects osteoblast functions pertinent to osteogenesis. *Annals of Biomedical Engineering*, 31(8):917–923, 2003. doi: 10.1114/1.1553454.
- R. D. O’Dea, S. L. Waters, and H. M. Byrne. A two-fluid model for tissue growth within a dynamic flow environment. *European Journal of Applied Mathematics*, 19(06):607–634, 2008. doi: 10.1017/s0956792508007687.
- R. D. O’Dea, S. L. Waters, and H. M. Byrne. A multiphase model for tissue construct growth in a perfusion bioreactor. *Mathematical Medicine and Biology*, 27(2):95–127, 2010. doi: 10.1093/imammb/dqp003.
- R. D. O’Dea, H. M. Byrne, and S. L. Waters. Continuum modelling of in vitro tissue engineering: a review. In L. Geris, editor, *Computational Modeling in Tissue Engineering*. Springer, 2012. doi: 10.1007/978-3-642-32563-2.
- G. Orlando, K. J. Wood, R. J. Stratta, J. J. Yoo, A. Atala, and S. Soker. Regenerative medicine and organ transplantation: past, present, and future. *Transplantation*, 91(12):1310–1317, 2011. doi: 10.1097/tp.0b013e318219ebb5.
- J. M. Osborne, R. D. O’Dea, J. P. Whiteley, H. M. Byrne, and S. L. Waters. The influence of bioreactor geometry and the mechanical environment on engineered tissues. *Journal of Biomechanical Engineering*, 132(5):051006+, 2010. doi: 10.1115/1.4001160.
- K. B. Paiva and J. M. Granjeiro. Bone tissue remodeling and development: focus on matrix metalloproteinase functions. *Archives of biochemistry and biophysics*, 561:74–87, November 2014. ISSN 1096-0384. URL <http://view.ncbi.nlm.nih.gov/pubmed/25157440>.
- J. Rauh, F. Milan, K. P. Günther, and M. Stiehler. Bioreactor systems for bone tissue engineering. *Tissue Engineering. Part B, Reviews*, 17(4):263–280, 2011. doi: 10.1089/ten.teb.2010.0612.
- S. C. Rawlinson, A. J. El-Haj, S. L. Minter, I. A. Tavares, A. Bennett, and L. E. Lanyon. Loading-related increases in prostaglandin production in cores of adult canine cancellous bone in vitro: a role for prostacyclin in adaptive bone remodeling? *Journal of bone and mineral research : the official journal of the American Society for Bone and Mineral Research*, 6(12):1345–1351, December 1991.
- R. C. Riddle and H. J. Donahue. From streaming-potentials to shear stress: 25 years of bone cell mechanotransduction. *Journal of Orthopaedic Research*, 27(2):143–149, February 2009. doi: 10.1002/jor.20723.
- N. Rivalain, J. Roquain, and G. Demazeau. Development of high hydrostatic pressure in biosciences: Pressure effect on biological structures and potential applications in Biotechnologies. *Biotechnology Advances*, 28(6):659–672, 2010. doi: 10.1016/j.biotechadv.2010.04.001.
- J. Roelofsen, J. Klein-Nulend, and E. H. Burger. Mechanical stimulation by intermittent hydrostatic compression promotes bone-specific gene expression in vitro. *Journal of Biomechanics*, 28(12):1493–1503, 1995.
- F. R. A. J. Rose and R. O. C. Oreffo. Bone Tissue Engineering: Hope vs Hype. *Biochemical and Biophysical Research Communications*, 292(1):1–7, 2002. doi: 10.1006/bbrc.2002.6519.
- J. E. Schroeder and R. Mosheiff. Tissue engineering approaches for bone repair: Concepts and evidence. *Injury*, 42(6):609–613, 2011. doi: 10.1016/j.injury.2011.03.029.
- M. A. Schwartz and R. K. Assoian. Integrins and cell proliferation: regulation of cyclin-dependent kinases via cytoplasmic signaling pathways. *Journal of Cell Science*, 114(Pt 14):2553–2560, 2001.
- E. Takai, R. L. Mauck, C. T. Hung, and X. E. Guo. Osteocyte viability and regulation of osteoblast function in a 3D trabecular bone explant under dynamic hydrostatic pressure. *Journal of Bone and Mineral Research : The Official Journal of the American Society for Bone and Mineral Research*, 19(9):1403–1410, 2004. doi: 10.1359/JBMR.040516.
- C. H. Turner. Three rules for bone adaptation to mechanical stimuli. *Bone*, 23(5):399–407, 1998. doi: 10.1016/s8756-3282(98)00118-5.
- V. W. Reong, K. C. Rustad, M. T. Longaker, and G. C. Gurtner. Tissue engineering in plastic surgery: a review. *Plastic and Reconstructive Surgery*, 126(3):858–868, 2010. doi: 10.1097/prs.0b013e3181e3b3a3.
- A. B. Yeatts and J. P. Fisher. Bone tissue engineering bioreactors: dynamic culture and the influence of shear stress. *Bone*,

- 48(2):171–181, 2011. doi: 10.1016/j.bone.2010.09.138.
- D. Zhang, S. Weinbaum, and S. C. Cowin. On the calculation of bone pore water pressure due to mechanical loading. *International Journal of Solids and Structures*, 35(34-35):4981–4997, December 1998a. doi: 10.1016/s0020-7683(98)00105-x.
- D. Zhang, S. Weinbaum, and S. C. Cowin. Estimates of the peak pressures in bone pore water. *Journal of Biomechanical Engineering*, 120(6):697–703, 1998b. doi: 10.1115/1.2834881.